

# Effect of Applied Pressure on Densification and Mechanical Properties of Sialon-ZrN Composites Fabricated Through a Reaction Bonding /Gas Pressure Sintering Process

L Yin<sup>1</sup> and M I Jones<sup>1,\*</sup>

<sup>1</sup> Department of Chemical and Materials Engineering, Faculty of Engineering, University of Auckland, Auckland 1023, New Zealand

\*mark.jones@auckland.ac.nz

**Abstract.** Sialon-ZrN composites have been produced by reaction bonding and gas pressure sintering, and the effects of applied pressure on the sintering and properties has been investigated. The results showed that composites were mainly composed of  $\beta$ -Sialon and ZrN, with intermediate phases (including  $Y_2SiAlO_5N$ ,  $Al_2SiO_5$  and  $Y_2Si_2O_7$ ) for 0.4 MPa and  $Y_5Si_4Al_2O_{17}N$  for 1.0 MPa. The mass loss decreased with pressure increase due to suppression of thermal decomposition of the Sialon. Composites sintered under 1.0 MPa had better densification than those sintered under 0.4 MPa, and presented greater mechanical properties. Under 1.0 MPa, compared to the monolithic Sialon, the addition of ZrN resulted in an increased hardness up to 30% ZrN, with the highest hardness of 16.16 GPa being observed with 20% ZrN. The hardness decreased with higher ZrN content due to the weak bonding between the ZrN particles and the Sialon matrix. However this resulted in a continuous increase in fracture toughness, reaching a maximum of 5.41 MPa·m<sup>1/2</sup> with 50% ZrN.

## 1. Introduction

Sialon is a group of compounds in the Si-Al-O-N system with a structure based on  $Si_3N_4$ , where Si-N bonds are partially replaced by Al-O bonds[1]. Sialon has been a promising ceramic material because of its excellent properties, such as high thermal shock resistance, high hardness, chemical inertness, good erosion resistance and low creep property[2,3]; and is widely used for bearings, heat exchangers, cutting tools, and refractories. Sialons are normally produced from expensively commercial  $Si_3N_4$ ,  $Al_2O_3$  and AlN powders. In order to reduce the raw material cost, a reaction bonding method using less inexpensive Si powders to replace the costly commercial  $Si_3N_4$  powders has been employed to fabricate Sialon materials. Conventional liquid phase reaction sintering, spark plasma sintering (SPS) and hot pressing sintering (HP) are the most common methods to fabricate high dense Sialon materials[4-6]. However, these methods require high temperature, high applied pressure and complicated equipment. SPS and HP are suitable for fabricating high density Sialon materials at a relatively low temperature in a short holding time, but they are not suitable for samples with complex shapes and large sizes. In recent research works gas pressure sintering (GPS) was shown to be suitable for mass production of Sialon/Sialon-based ceramics and other ceramics as a laboratory and industrial technique[7,8]. During the densification of Sialon and Sialon-based ceramics, the decomposition of Sialon can result in negative effects on the sintering behavior and properties of the materials. For the GPS technique, a high nitrogen gas pressure can prevent the decomposition of Sialon and also provide



an extra driving force for the sintering which helps to lower the sintering temperature and the amount of sintering additives required. The sintering of Sialon and Sialon-based ceramics produced by GPS, is not ascertained by a single factor, but is influenced by several factors[9,10], such as sintering temperatures, gas pressures, compositions of the gas and sintering additive contents.

In previous work[11], we have discussed the effect of sintering temperature on the sintering behavior and properties of Sialon-ZrN composites. In the current work, we have investigated the effect of the applied nitrogen gas pressure on the densification and mechanical properties of the  $\beta$ -Sialon-ZrN composites. The scope of this work was to determine an available pressure range to obtain high density Sialon-ZrN composites with satisfactory hardness and fracture toughness.

## 2. Experiment Work

The starting composition of the composites consisted of pre-synthesized  $\beta$ -Sialon ( $z=1$ ) powders (details of the preparation process have been described in previous work[11]), and commercial ZrN powders (Sigma-Aldrich Ltd., D50 $\approx$ 3  $\mu$ m). The ZrN content was varied from 0% to 50 wt% in increments of 10 wt%. Sintering additives were composed of  $Y_2O_3$  and  $Al_2O_3$  with a molar ratio of 3:5 (i.e. YAG composition), and a total amount of 8 wt%. The powder mixtures were ball-milled in isopropanol for 4h with  $Si_3N_4$  balls, then dried in a rotary evaporator and passed through a 250  $\mu$ m sieve. The sieved powders were uniaxially pressed into pellets, and cold isostatically pressed at 200 MPa for 5 min. The green compacts were placed into a BN crucible and sintered in a high temperature graphite furnace at 1700  $^{\circ}C$  for 6h under an nitrogen pressure of 0.4 and 1.0 MPa, respectively.

Following sintering, bulk densities and open porosities of the ground and polished samples were determined by the Archimedes' method. Relative density was determined by comparison to the theoretical density of the composites determined from a rule of mixtures for each composition.

The phase assemblages of the sintered samples were analyzed by XRD diffraction. The morphologies were observed with a field-emission gun scanning electron microscope (ESEM, FEI QUANTA 200, USA). Vickers hardness (according to ASTM C1327-15 [12]) and indentation fracture toughness were measured using a Vickers hardness tester equipped with a diamond indenter on the polished surface with a 98 N load for 15 s. Fracture toughness was calculated by the following equation as described by G. R. Anstis et. al[13] :

$$K_{IC} = (0.016 \pm 0.004) \times \left( \frac{E}{H_V} \right)^{0.5} \times \left( \frac{P}{c^{3/2}} \right) \quad (1)$$

where  $H_V$  is the Vickers hardness,  $c$  is the crack length, and  $E$  is the Young's modulus for the composites calculated by rule of mixtures.

## 3. Results and discussions

### 3.1. Influence of applied pressure on phase assemblage and microstructure of the sintered composites

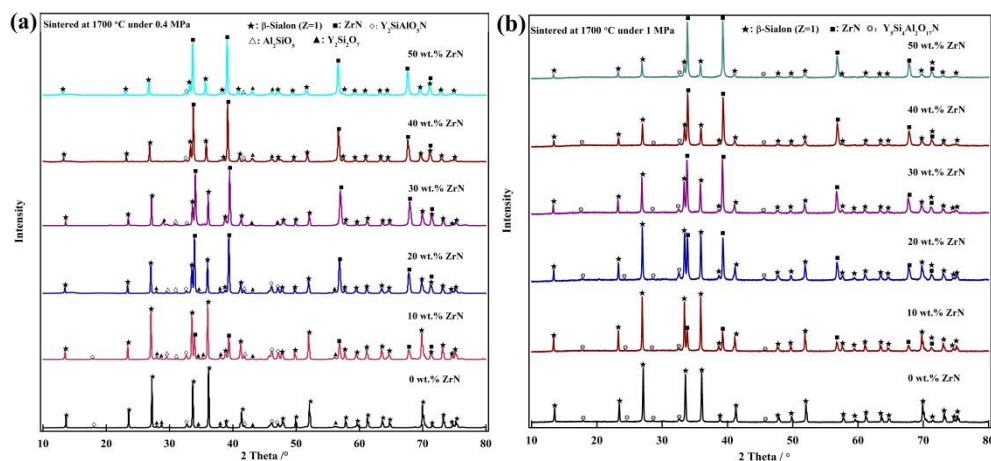


**Figure 1.** The XRD patterns of the composites sintered at 1700 °C under nitrogen pressure of (a) 0.4 and (b) 1.0 MPa for 6 h, respectively.

Figure 1 shows the phase assemblage of the composites sintered at 1700 °C under applied nitrogen gas pressure of 0.4 and 1.0 MPa, respectively. According to the XRD results, under these two pressures, the composites were mainly composed of  $\beta$ -Sialon and ZrN, with secondary phases of  $Y_2SiAlO_5N$ ,  $Al_2SiO_5$  and  $Y_2Si_2O_7$  for 0.4 MPa (shown in figure 1(a)), while only  $Y_5Si_4Al_2O_{17}N$  was observed in samples produced under 1.0 MPa shown in figure 1(b). These results show that variation in applied pressure had no influence on the major phases, while it affected the formation of minor phases. For this sintering process, the nitrogen pressure mainly served as an external pressure to assist the densification of composites, and it had limited influence on their phase assemblage.

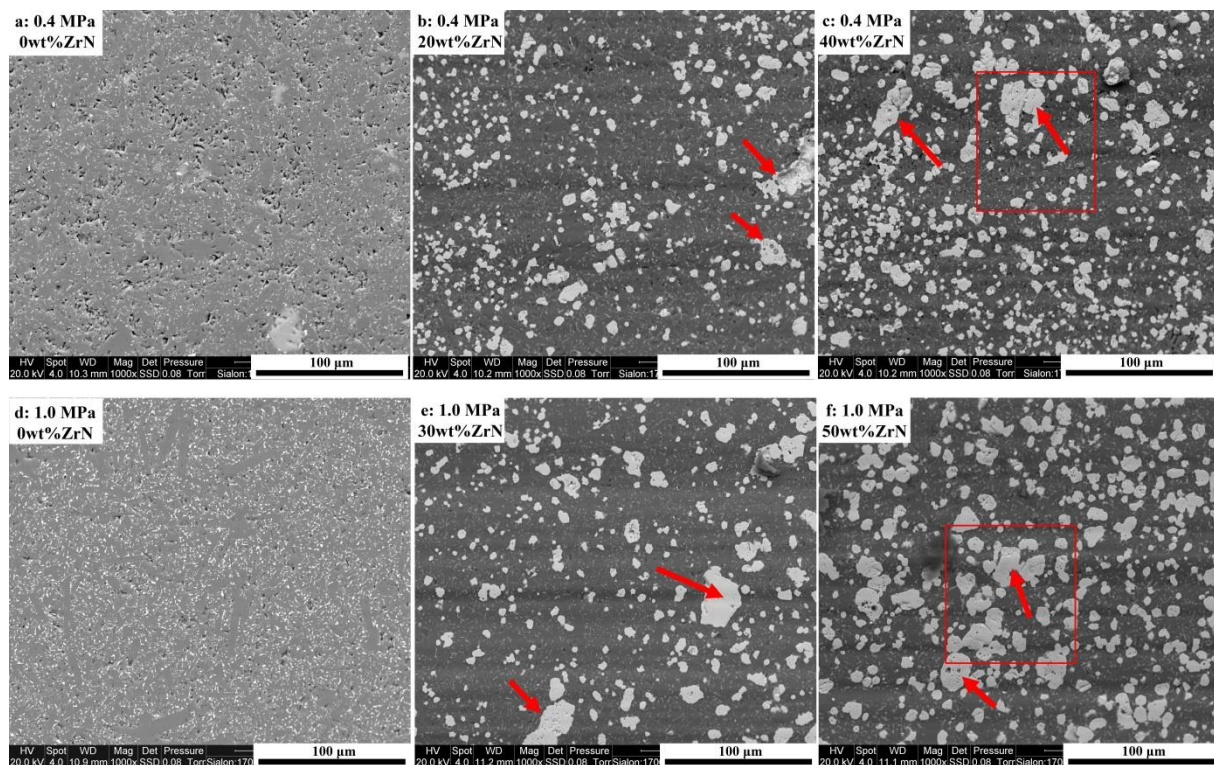
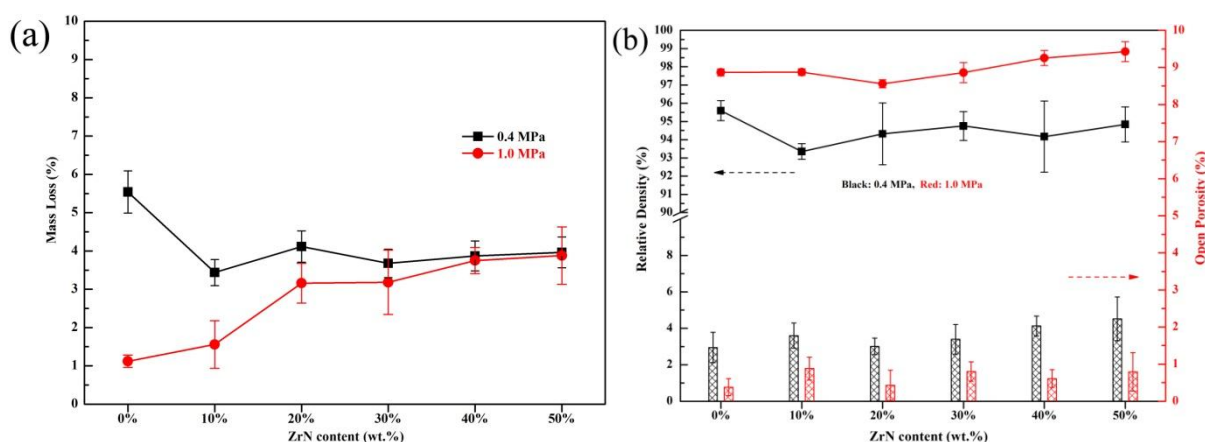


**Figure 2.** The morphologies of the composites sintered at 1700 °C under nitrogen pressure of 0.4MPa and 1.0 MPa, respectively.

During gas pressure sintering, pressure also plays an important role on grain growth, pore elimination and grain boundary mobility, leading to differences in the microstructure of the composites, as shown in Figure 2. As can be seen in Figures 2a and 2d, the monolithic Sialon sintered under 0.4 MPa had more residual pores with larger sizes than those under 1.0 MPa. As shown in Figure 2d, a larger number of high aspect ratio  $\beta$ -SiAlON ( $Z=1$ ) grains were observed under a nitrogen gas pressure of 1.0 MPa. For all of the samples, the amount of pores decreased with increase in ZrN content due to the ZrN particles distributing into the grain boundaries to affect the boundary mobility. For the composites sintered under these two applied pressures, abnormal grain growth of the ZrN particles (red arrows) was found and some pores became trapped within the surface of ZrN particles.

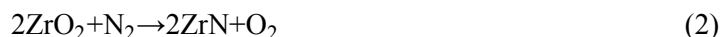
### 3.2. Influence of applied pressure on densification behaviour of the sintered composites





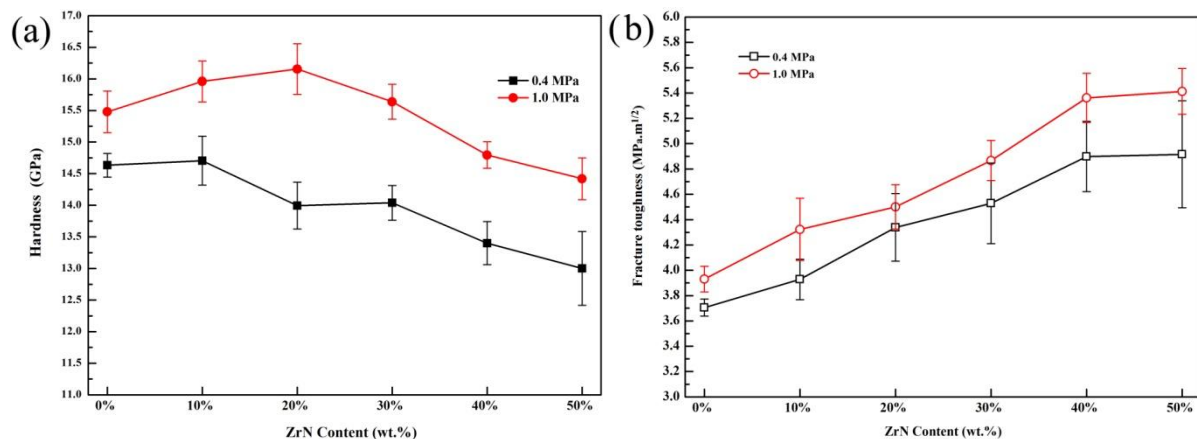
**Figure 3.** Effect of nitrogen pressures on (a) mass loss, (b) relative density and open porosity of composites with different ZrN contents sintered at 1700 °C for 6h.

Figure 3a shows the mass loss of composites sintered at 1700 °C under a nitrogen pressure of 0.4, and 1.0 MPa, respectively. The results indicated that composites sintered under low pressure (0.4 MPa) had the highest mass loss, and this decreased with increase in nitrogen pressure. For Sialon-ZrN composites, the thermal decomposition of Sialon matrix was the predominant reason for mass loss. The results in Figure 3a show that this thermal decomposition of  $\beta$ -SiAlON is affected by the magnitude of the gas pressure. It has been shown that the partial pressure of SiO is important for the stability of  $\beta$ -SiAlON[14]. If it is assumed that  $P_{N_2} + P_{SiO} = 1$  atm, at 1800 °C, the single phase  $\beta$ -SiAlON would be stable when the SiO partial pressure was between 0.39 and 0.60 atm. During the decomposition process of  $\beta$ -SiAlON, SiO gas could escape from the bulk sample under a low sintering atmosphere pressure. This could decrease the partial pressure of SiO in the bulk sample, leading to further thermal decomposition of Sialon. Increasing pressure makes it more difficult for SiO gas to diffuse out the sample, causing the increased SiO partial pressure to halt thermal decomposition of Sialon, finally resulting in less mass loss. High pressure is believed to result in suppression of the thermal decomposition of the Sialon matrix, resulting in the decreased mass loss with pressure. Under a nitrogen pressure of 0.4 MPa, the mass loss of composites was lower than that of monolithic Sialon and varied slightly with increase in ZrN content. However, under high nitrogen pressure of 1.0 MPa, the mass loss increased with increasing ZrN content, reaching around 4% for a ZrN content of 50%. For the commercial ZrN powders,  $ZrO_2$  is an unavoidable oxide existing on the surface of the ZrN particles. A reaction between  $ZrO_2$  and ZrN could take place by the following equation, leading to the slight increase in mass loss with ZrN content.



The relative density and open porosity of the composites sintered at 1700 °C under applied pressure of 0.4 and 1.0 MPa are presented in Figure 3b. The results show that the composites sintered under low pressure had poorer densification behavior with relative density around 93% and open porosity between 1.5 to 3%. The composites sintered under high pressure (1.0 MPa) had greater densification behavior, where the relative densities reached 98% and open porosities were less than 1.5%, indicating that increasing pressure was beneficial for the densification. This was because the densification occurred by diffusional processes under the influence of surface energy as a driving force. The driving force increased with applied pressure and resulted in higher relative density and low open porosity. However, during the sintering, it was impossible to avoid thermal decomposition of the Sialon matrix, the formation of intermediate phases and the existence of residual closed pores located at grain-boundary intersections, indicating the difficulty in obtaining 100% full dense composites.

### 3.3. Influence of applied pressure on the hardness and fracture toughness of the sintered composites



**Figure 4.** The (a) hardness and (b) fracture toughness of the  $\beta$ -Sialon-ZrN composite with different ZrN contents sintered at 1700 °C under a nitrogen gas pressure of 0.4 and 1.0 for 6h.

Figure 4 presents the hardness (HV10) and indentation fracture toughness of the  $\beta$ -Sialon-ZrN composite with different ZrN contents sintered at 1700 °C under a nitrogen gas pressure of 0.4 and 1.0 for 6 h. The results in this figure demonstrate that it is possible to improve the mechanical properties of the Sialon matrix composites through a combination of increase in applied pressure and amount of reinforcing phase. As shown in figure 4(a), the highest hardness for samples sintered under a high gas pressure (1.0 MPa) regardless of ZrN content, thought to be due to the higher density of these samples (shown in figure.3b). Under 1.0 MPa, compared to the sample with no reinforcement, the addition of ZrN resulted in an increased hardness up to a ZrN content of 30 wt%, with the highest hardness around 16.10 GPa being observed with 20 wt% ZrN; The hardness decreased for higher ZrN content, but this was not related to density since they were similar for all samples. The similar effect of secondary phase on hardness of Sialon-matrix composites has been observed in Y- $\alpha$ -Sialon-cBN composites, and was attributed to weak bonding between the matrix grains and the reinforcing particles [15]. In the present work, such weakening may also have been observed, due to the differences in thermal expansion coefficients of the two materials and/or the residual stresses due to the differences in sinterability of the two materials, normally densification of ZrN being obtained at higher than 2000 °C (much higher than fully densification of Sialon matrix)[16]. This weakening is increased with increasing amounts of ZrN, since the distribution of ZrN grains tends towards a continuous network, softening the composite and resulting in the decrease in hardness. Again as can be seen in figure 4(b), the samples sintered under high pressure (1.0 MPa) had the greater fracture toughness due to the higher density and lower amount of porosity. Unlike hardness, which went through a maximum with increasing ZrN content, the fracture toughness increased continuously up to a value of 5.40 MPa·m<sup>1/2</sup> for 50 wt% ZrN. The crack paths and toughening mechanisms of the composites are shown in Figure 5, where all of the toughening mechanisms known in ceramic materials can be observed (i.e. crack branching, crack deflection and crack bridging) [17,18].

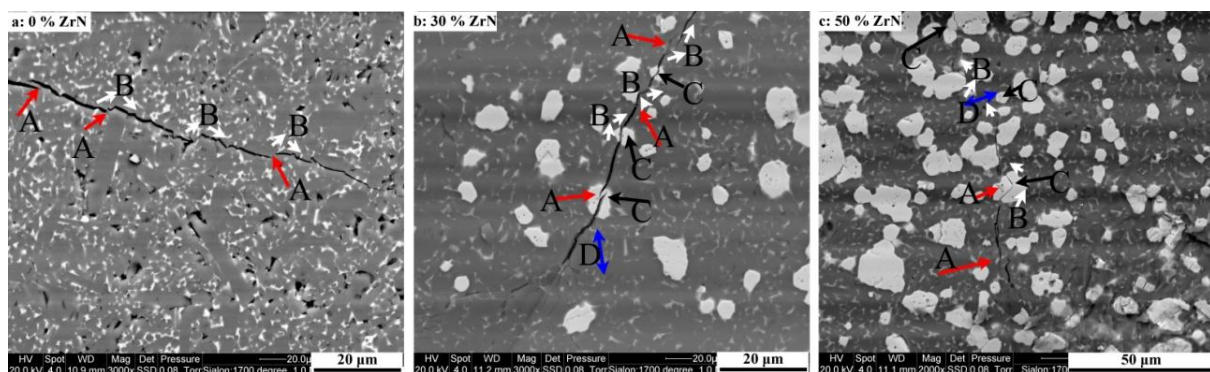


**Figure 5.** The crack paths and toughen mechanisms being observed in the selected composites, including the crack deflection (B-white arrows), crack bridging (A-red arrows), transgranular fracture (C-black arrows) and crack branching (D-blue arrows)

Generally, for  $\text{Si}_3\text{N}_4$  and  $\text{Si}_3\text{N}_4$ -based materials, the composition and microstructure (i.e grain size and shape, grain boundary phases and reinforcing phases) have great effect on the fracture toughness, as described by numerous works[19-21]. As can be seen in Figure 5, for the monolithic Sialon material, the fracture toughness was predominantly influenced by crack bridging and crack deflection. With increasing in ZrN content, more crack deflection and crack branching were observed due to ZrN particles distributed into the grain boundaries and triple junctions and the more weaker interfaces between the matrix and the reinforcing phase. Also it needed more energy to break the higher ZrN particles than the Sialon matrix. These phenomena all consume energy and/or make the propagation of cracks more difficult, and lead to the increased toughness. Although the weaker interface with increasing ZrN results in decreasing hardness when the amount of reinforcement is increased, it allows for more crack bridging and crack deflection, and thus results in a higher toughness.

#### 4. Conclusions

The influence of applied nitrogen gas pressure on the densification and properties of Sialon-ZrN composites have been investigated through a reaction bonding /post sintering process. Composites sintered under nitrogen pressures of 0.4 and 1.0 MPa were composed of an elongated  $\beta$ -Sialon ( $Z=1$ ) matrix, and equiaxed ZrN particles, with intermediate phases (including  $\text{Y}_2\text{SiAlO}_5\text{N}$ ,  $\text{Al}_2\text{SiO}_5$  and  $\text{Y}_2\text{Si}_2\text{O}_7$ ) for 0.4 MPa and  $\text{Y}_5\text{Si}_4\text{Al}_2\text{O}_{17}\text{N}$  for 1.0 MPa. The composites sintered under higher nitrogen gas pressure (1.0 MPa) had less mass loss due to the suppression of the thermal decomposition of  $\beta$ -Sialon, and also showed greater densification with a relative density around 98% and small open porosity less than 1.5%. These samples achieved the higher hardness and fracture toughness, which were both affected by the ZrN content. The hardness of the composites reached a maximum ( $16.16 \pm 0.40$  GPa) at 20 wt% ZrN and decreased for higher contents, due to weakly bonded interfaces between the Sialon matrix and the ZrN particles. The reinforcing ZrN phase helped to toughen the composite by different toughening mechanisms, such as crack deflection, crack bridging, transgranular fracture and crack branching. The addition of ZrN promoted a continuous increase in fracture toughness of the composites, where the maximum fracture toughness of  $5.41 \pm 0.18$  MPa·m<sup>1/2</sup> was observed with 50 wt% ZrN. This work indicates that increase in the applied gas pressure in GPS technique was positive for the densification and mechanical properties of Sialon and Sialon-based ceramics and an appropriate content of a reinforcing phases was beneficial for the densification and properties of Sialon materials.

#### Acknowledgements

Li Yin would like to acknowledge the China Scholarship Council (CSC) for providing a doctoral scholarship. The authors are grateful to technical staff in the Chemical & Materials Engineering Department at the University of Auckland for their assistance with preparation, property testing and data analysis.

#### References

- [1] Liu H Tao, Meng F Rong, Li Q, Huang Z Hui, Luo S Qin, Yin L, Fang M Hao, Liu Y Gai and Wu X Wen 2015 *Cryst. Eng. Comm* **17** 1591
- [2] Rueanngoen A, Kanazawa K, Akiyoshi M, Imai M, Yoshida K and Yano T 2013 *J. Nucl. Mater* **442** S394
- [3] Li Y jun, Yu H Liang, Jin H Yun, Liu D Hua, Qiao G Jun, Jin Z Hao and Shi Z Qi 2014 *J. Alloy. Compd* **616** 639.
- [4] Khan M A Raja, Malki M A Moath, Hakeem S Abbas, Ehsan A Muhammad and Laoui T 2016 *Mater. Sci. Eng. A* **673** 243
- [5] Nekouee A Kh and Khosroshahi R A 2016 *Int. J. Refract. Met. H* **61** 6

- [6] Abo-Naf S M, Dulias U, Schneider J, Gahr K H Z, Holzer S and Hoffmann M J 2007 *J. Mater. Process. Tech* **183** 264
- [7] Liu S Chao, Ye F, Hu S Qing, Yang H Xia, Liu Q and Zhang B 2015 *J. Alloy. Compd* **647** 686
- [8] Rocha V Cláudio and Costa A C d'io 2006 *Materials Research*. **9** 143
- [9] Hyuga H, Yoshida K, Kondo N, Kita H, Sugai J, Okano H and Tsuchida J 2009 *Ceram. Int* **35** 1927
- [10] Li Y, Liu D, Zeng C, Shi Z and Jin Z 2016 *J. Mater. Eng. Perform* **25** 1143
- [11] Yin L and Jones I Mark 2018 *Ceram. Int*. In press
- [12] ASTM C 1327-15, *ibid*, vol. **15**.01
- [13] Anstis G R, Chantikul P, Lawn B R and Marshall D B 1981 *J. Am. Ceram. Soc* **64** 533
- [14] Mitomo M, Kuramoto N and Yajima Y 1980 *Journal of the Ceramic Association, Japan*. **88** 49
- [15] Garrett J C, Sigalas I, Herrmann M, Olivier E J and O'Connell J H 2013 *J. Eur. Ceram. Soc.* **33** 2191
- [16] Li D, Yang Z, Jia D, Hu C, Liang and Zhou Y 2015 *J. Eur. Ceram. Soc* **35** 4399
- [17] Steinbrech R W 1992 *J. Eur. Ceram. Soc* **10** 131
- [18] Ritchie O Robert 1988 *Mater. Sci. Eng. A* **103** 15
- [19] Björklund H, Falk L K L, Rundgren K and Wasén J 1997 *J. Eur. Ceram. Soc* **17** 1285
- [20] Becher F Paul, et al 1998 *J. Am. Ceram. Soc* **81** 2821
- [21] Blugan G, Hadad M, Janczak-Rusch J, Kuebler J and Graule T 2005 *J. Am. Ceram. Soc* **88** 926